Image Quality Evaluation of Chest for Computed Radiography

A.F.VELO[1], D.R.PINA[2], S.B.DUARTE[3], M.ALVAREZ[1], M.OLIVEIRA[1], S.M.RIBEIRO[2] and J.R.MIRANDA[1]

[1] Instituto de Biociências de Botucatu/Departamento de Física e Biofísica, UNESP, Botucatu, Brasil
[2] Faculdade de Medicina de Botucatu/Departamento de Doenças Tropicais e Diagnóstico por Imagem, UNESP, Botucatu, Brasil
[3] Centro Brasileiro de Pesquisas Físicas, CBPF, Rio de Janeiro, Brasil

Abstract— **The daily-to-day of medical practice is marked by a constant search for an accurate diagnosis and therapeutic assessment. For this purpose the doctor serves up a wide variety of imaging techniques, however, the methods using ionizing radiation still the most widely used because it is considered cheaper and above all very efficient when used with control and quality. The optimization of the risk-benefit ratio is considered a major breakthrough in relation to conventional radiology, though this is not the reality of computing and digital radiology, where Brazil has not established standards and protocols for this purpose. This work aims to optimize computational chest radiographs (anterior-posterior projection-AP). To achieve this objective were used a homogeneous phantoms that simulate the characteristics of absorption and scattering of radiation close to the chest of a patient standard. Another factor studied was the subjective evaluation of image quality, carried out by visual grading assessment (VGA) by specialists in radiology, using an anthropomorphic phantom to identify the best image for a particular pathology (fracture or pneumonia). Quantifying the corresponding images indicated by the radiologist was performed from the quantification of physical parameters (Detective Quantum Efficiency – DQE, Modulation Transfer Function – MTF and Noise Power Spectrum - NPS) using the software MatLab®.**

Keywords— **Computed Radiography, Visual Grading Assessments, Modulation Transfer Function, Noise Power Spectrum, Detective Quantum Efficiency.**

I. Introduction

It has been proposed in the last decades, as detectors of radiation, the alternative use of radiographic films. These new transducers are associated with digital imaging systems. In this mode of obtaining the image, a reusable sensor absorbs radiation generating an electrical signal or light, which is digitized and transferred to a microcomputer, where the images are reconstructed, stored and displayed [1,2]. The integration of radiology computing market forms the basis for a filmless radiology service. Filmless radiology refers to a hospital which has a comprehensive and integrated network environment whose film was completely or largely replaced by electronic systems that acquire, archive, make available and display images [3,4]. This new technology helps to reduce the repetition of exams, which carries an unnecessary financial expense for the institution and harm to patients by the additional radiation provided by the excess of repeated examinations.

The optimization of cost and risk-benefit ratio is a part of the main objectives of a Quality Control Program (QCP) and should be carefully considered especially in relation to the thoracic radiology [5]. The chest X-ray is the most accomplished by the world's population. Each individual carries at least one chest x-ray during life, especially for diseases related to respiratory problems [6]. At the Hospital of Clinics of Botucatu (UNESP-HCFMB) are performed on average two thousand chest x-rays per month. However, nowadays, there are few institutions that have letters of radiographic techniques for conducting examinations as requested by current standards [7]. Dealing with computational radiology may be considered a gap in the clinical routine, because institutions that use this method of diagnostic imaging employ the same techniques of image production of screen-film system. It is important to note that the exiting national rules do not describe protocols to be used in the process of optimization of computed images. The protocols used to optimize this method of diagnostic imaging are based on international protocols [8]. Within this context, we propose in this research to optimize images of the chest for Computed Radiography (CR) as contributions to the construction of protocols for optimizing images for different pathologies (pneumonia and fracture) to be implemented in clinical routine, supplying a gap in the radiology sectors that employ this method of diagnostic imaging.

II. Methodology

To achieve the purposed objective, were determined images of CR obeying the logarithmic mean exposure (lgM) which by definition has a value of 1.96 for any Speed Class (SC) applied [9,10], however was established for the research a variation of lgM from 1.8 to 2.0, because the reference is recommended by the manufacturer.

lgM is a feedback response appropriate to the level of exposure in the clinical routine, so it indicates how closely the dose used in the detector is to the expected dose. The

M. Long (Ed.): World Congress on Medical Physics and Biomedical Engineering, IFMBE Proceedings 39, pp. 2308–2311, 2013.
www.springerlink.com

determination of SC and the radiographic technics such as Kilovoltage peak (kVp), the Milliamperage x time (mAs) and Source - Filme Distance (SFD), associated with IgM were purchased from the assessment of the SC and the calibration of the X-ray beam respectively.

The equipments used for this research was the Siemens model: 844002, Agfa HealthCare 85-X and the ionizing chamber Radcal 9015.

A. SC Evaluation

The term speed indicates for the system the expected value of signal on imaging plate (IP). It means that, if chosen a low SC, the signal expected that will achieve the detector is high, so it decreases the sensibility and the gain factor on the photomultiplier tube and them the signal recognized will be low. Conversely if the SC is high, the opposite will happen, therefor these chances on SC shift the histogram of the image, and if chosen an incoherent SC it may compromise the quality of the image [11].

To analyze the SC were used an homogeneous phantom (PEP) figure 1.a, and varied the SC on 100, 200, 400 and 800 and on each image of the PEP was applied the NPS in order to check whose presented a less noisy comportment. The determination of NPS will be presented on section E.

B. *Calibration of the beam and dosimetric systems and images evaluation*

In the procedure of calibration of the x-ray beam, the images were scanned using SC 400. The PEP was used to calibrate the x-ray beam with the dosimetric system. Figure 1.a shows the schematic illustrative of the calibration proceedings.

On this proceedings it was selected a voltage range of 70 – 120 kVp, with step of 5 kVp, aperture field 30 x 30 cm and SFD of 180 cm. The mAs are related with the lgM.

Each value of kVp was associated with a determined mAs in order to verify the corresponding lgM. So it was obtained about four mAs values for each kVp. Forward was built a relationship between Kerma (Kinetic Energy Released in Matter) and signal to noise ratio (SNR). On this step the PEP was replaced by an ionizing chamber, with the purpose to register the corresponding kerma of each techniques, then, on each image was selected a region of interest (ROI) to estimate the SNR.

The techniques selected on this proceeding were applied on an anthropomorphic phantom, figure 1.b, and the images were evaluated by a specialist of the radiology area for different pathologies (fracture and pneumonia). On this proceeding it was used the Visual Grading Analysis (VGA) [12,13].

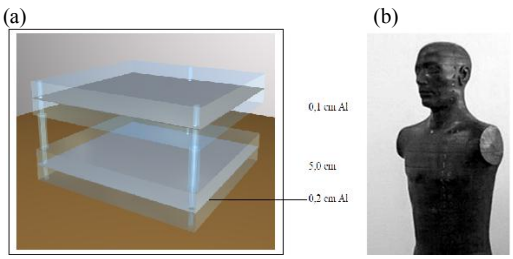

Fig. 1 Homogenous Phantom a), Anthropomorphic Phantom b).

C. Objective Evaluation of Image

At this stage of the research was quantified the physics parameters associated with the selected images indicated by the radiologist. This quantification was performed using an Analitic-Realistic phantom (RAP-PEP), shown on figure 2 [12,13,14,15]. This phantom was x-rayed with the techniques previously determined, described on section B. From the images of the RAP-PEP the physics parameters evaluated: MTF, NPS and DQE.

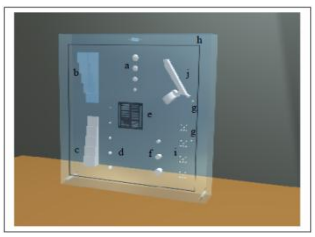
Fig 2 Analitic-Realistic Phantom

D. MTF Measurement

The acquisition of MTF was performed by the edge method [16]. To achieve this purpose, it was selected a ROI of the resolution board presented on the RAP-PEP, that contains an edge and them was applied the Hough transformed to determine the angulation of this edge and corrected so that the edge gets 90 degrees. Them was performed the average of each column of the ROI obtaining the Edge Spread Function (ESF), vectoring the image. This vector was derived to obtain the Line Spread Function (LSF). So applying the Fourier Transform (FFT) the MTF was measured to quantify the resolution of the system.

E. DQE Measurement

The frequency-dependent bin NPS (f), is defined as the variance per frequency bin of a stochastic signal in the spacial frequency domain. Although it may be computed as the Fourier Transform of the autocovariance function by use of the Wiener-Kintchin Theorem, the NPS is most commonly computed directly from the square Fourier amplitude of two-dimensional image data using [17]:

$$\text{NPS}(u_n, v_k) = \lim_{NxNy\to\infty}(NxNy\Delta x\Delta y)\langle|\text{FTnk}[I(x,y)-\bar{I}]|^2\rangle$$
$$= \lim_{NxNy\to\infty}\lim_{M\to\infty}\frac{NxNy\Delta x\Delta y}{M}\sum_{m=1}^{M}\langle|\text{FTnk}[I(x,y)-\bar{I}]|^2 \quad (1)$$
$$= \lim_{NxNyM\to\infty}\frac{\Delta x\Delta y}{M.NxNy}\sum_{m=1}^{M}\left|\sum_{i=1}^{Nx}\sum_{j=1}^{Ny}[I(xi,yj)-\bar{I}]e^{-2\pi i(u_n xi+vkyi)}\right|^2$$

The NPS is often used as an input to the computation of detective quantum efficiency (DQE). In the DQE computation, it is necessary to correct for the gain of the system, and the NPS (given in units of digital value squared times mm^2) is divided by the square of the mean value of the pixels used for analysis (in units of digital value). This ratio is referred to as the normalized noise power spectrum (NNPS), and has units of mm^2:

$$\text{NNPS}(u,v) = \text{NPS}(u,v)/(\text{large area signal})^2 \quad (2)$$

The frequency-dependent DQE (f) is now able to be computed [18]:

$$\text{DQE (f)} = S^2\frac{MTF^2(f)}{NPS(f)XqXE} = \frac{MTF^2(f)}{NNPS(f)XqXE} \quad (3)$$

where $MTF(f)$ is the frequency-dependent MTF, $NPS(f)$ is the frequency-dependent NPS, $NNPS(f)$ is the frequency-dependent normalized NPS, E is an estimated value of the men pixel value to an exposure value and q an estimated value by means of computed spectrum modeling of the beam conditions evaluated.

F. Implementation of the optimized technical equipment to other conventional X-ray, using the same CR system

One way to achieve equivalence of quality of the beam is from the half-value layer (HVL) and the intensity of the beam from the equation 4 [14].

$$mAs_2 = \frac{R_1BF_1}{R_2BF_2}mAs_1 \quad (4)$$

where the index 1 described on equation 4 are given to the equipment where the techniques were optimized, while the index 2 refers to the equipment where the techniques will be implement, R means the efficiency of the equipment and the BF means the Bucky Factor.

III. Results

In the analysis of which SC would provide a behavior less noisy, the SC 400 appeared to be better than the others, figure 3, so all images were acquired using this SC.

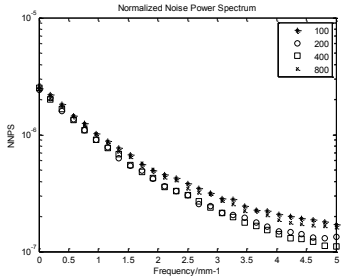

Fig. 3 Normalized Noise Power Spectrum for SC.

Figure 4 represent the ESF evidencing the edge selected by the ROI, figure 5 show the LSF obtained by the derivation of ESF, and then applying the FFT was measured the MTF as shown on figure 6.

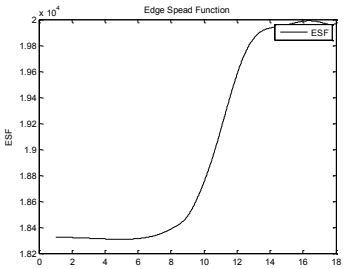

Fig. 4 Edge Spread Function

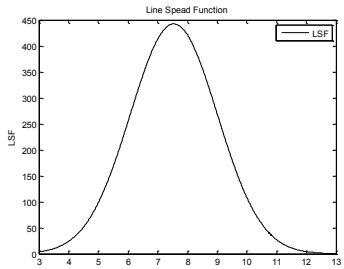

Fig. 5 Line Spread Function

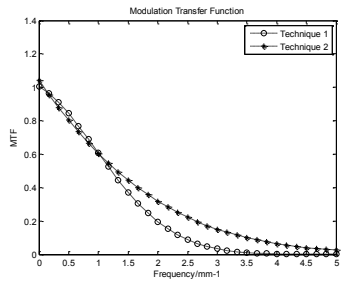

Fig. 6 Modulation Transfer Function of 2 techniques selected

For acquire the DQE, first was necessary obtain the NPS through equation 1 and normalize it by equation 2, the results of NNPS is show on figure 7. After obtained the NNPS we measured the DQE, by equation 3, and the results of DQE are on figure 8.

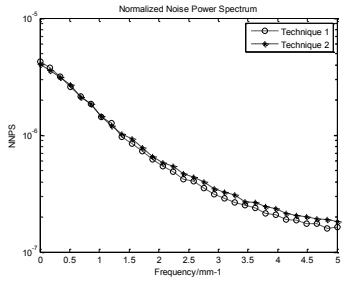

Fig. 7 Normalized NPS

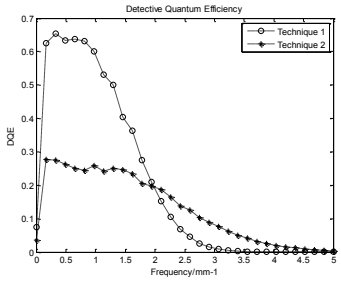

Fig 8 Detective Quantum Efficiency

Figure 9 shows the implementation of the optimized techniques to another CR system.

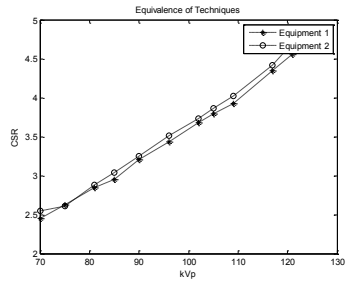

Fig. 9 Equivalence of techniques

IV. CONCLUSIONS

From the development of the physics parameters purposed on this research along with the choices made by the radiologist , it was possible to compare the images regarded as best qualities by both methods and optimize these techniques with that whose submitted lower dose, complying the main of this research.

ACKNOWLEDGMENT

The laboratory of physics applied to the radiodianostic, the laboratory of Biomagnetism and the financial support agency CAPES.

REFERENCES

1. Beird, L C., (May) 1999, The Importance of a Picture Archiving and Communications System (PACS) Manager for Large-Scale PACS Installations. Journal of Digital Imaging, Vol. 12, p. 37..
2. Siegel E L, Kolodner R M. 1999, Filmless Radiology: State of the Art and Future Trends - in Filmless Radiology. Springer-Verlag, pp. 3-20.
3. Freech D, Baune M., (May) 1999, The Process of Convertig to a Near Filmless Operation at the University of Utah. Journal of Digital Imaging, Vol. 12, pp. 41-46.
4. Siegel E L, Reinner B I., (May) 1999, Challenges Associated with the Incorporation of Digital Radiography into a Picture Archival and Communication System .Journal of Digital Imaging, Vol. 12, pp. 6-8.
5. Ratcliffe J, Swanson C E , Hafiz N, Frawley K, Coakley K, Cloake J. 2003, Assessment of image quality of a standard and two dose-reducing protocols in paediatric pelvic CT. Pediatr Radiol, Vol. 33, pp. 177-182.
6. Pina D R, Duarte S B, Ghilardi Netto T, Trad C S, Brochi M A C, Oliveira S C de. 2005, Radiographic image optimization of skull, pelvis and chest for non-standar patients. Phys Med Biol.
7. Anvisa. Portaria/MS/SVS nº 453. 1998.
8. American Association of Physcis in Medicine. Acceptance Testing and Quality Control of Photostimulable Storage Phosphor Imaging Systems. 2006. AAPM Repourt Nº93
9. Schaetzing, Ralph. 2004, Management of pediatric radiation dose using Agfa computed radiography. Pediatr Radiol, Vol. 34, pp. 207–214.
10. C S MOORE, BSc, MSc, J R SAUNDERSON, BSc, MSc and A W BEAVIS, BSc, PhD. 2009, Investigating the exposure class of a computed radiography system for optimisation of physical image quality for chest radiography.The British Journal of Radiology, Vol. 82, pp. 705–710.
11. Pina, D.R. Metodologia para otimização de imagens radiográficas. Tese (Doutorado) Faculdade de Filosofia, Ciências e Letras, Universidade de São Paulo. Ribeirão Preto : s.n., 2002.
12. Pina D R, Ghilardi Netto T, Rocha S L, Brochi M A C, Trad C S. 2000, Construção de um fantoma homogêneo para padronização de imagens radiográficas.Radiol Bras, Vol. 33, pp. 41-44.
13. Pina D R, Duarte S B, Ghilardi Netto T, Trad C S, Brochi M A C, Oliveira S C de. 2004, Optimization of standard patient radiographic images for chest, skull and pélvis exams in conventional x-ray equipment. Phys Med Biol , Vol. 49, pp. 215-226.
14. c. Pina D R, Morceli J, Trad C S, Ghilardi Netto T, Duarte S B, Oliveira S C. 2005, Development and construction of phantom for image optimizaton of skull and chest in lateral projection. Phys Med Biol .
15. Samei E., J.T. Dobbins III,, N. T. Ranger, Y. Chen. (May) 2006, Intercomparison of the methods for image quality characterization. I.Modulation Tranfer Function a) .Med. Phys, Vol. 33, pp. 1466-1475.
16. Dobbins III J., Samei E., Ranger N., Chen Y. 2006, Intercomparison of methods for image characterization. II. Noise power spectrum b).Med Phys. , Vol. 33 .
17. Ranger N., Samei E., Dobbins J., Ravin C. 2007, Assessment of detective quantum efficiency: Intercomparison of a recently introduced internacional standard with prior methods. Radiology.

Author: Alexandre França Velo
Institute: Instituto de Biociências de Botucatu
Street: Distrito de Rubião Jr., s/nº
City: Botucatu
Country: Brasil
Email:afvelo@ibb.unesp.br